**Atmospheric
Chemistry
and Physics**

Regional N$_2$O fluxes in Amazonia derived from aircraft vertical profiles

M. T. S. D'Amelio[1], **L. V. Gatti**[1], **J. B. Miller**[2,3], **and P. Tans**[2]

[1]Instituto de Pesquisas Energéticas e Nucleares (IPEN), São Paulo, Brazil
[2]National Oceanic and Atmospheric Administration (NOAA), Colorado, USA
[3]Cooperative Institute for Research in Environmental Sciences (CIRES), University of Colorado, Colorado, USA

Abstract. Nitrous oxide (N$_2$O) is the third most important anthropogenic greenhouse gas. Globally, the main sources of N$_2$O are nitrification and denitrification in soils. About two thirds of the soil emissions occur in the tropics and approximately 20% originate in wet rainforest ecosystems, like the Amazon forest. The work presented here involves aircraft vertical profiles of N$_2$O from the surface to 4 km over two sites in the Eastern and Central Amazon: Tapajós National Forest (SAN) and Cuieiras Biologic Reserve (MAN), and the estimation of N$_2$O fluxes for regions upwind of these sites. To our knowledge, these regional scale N$_2$O measurements in Amazonia are unique and represent a new approach to looking regional scale emissions. The fluxes upwind of MAN exhibited little seasonality, and the annual mean was 2.1±1.0 mg N$_2$O m^{-2} day^{-1}, higher than that for fluxes upwind of SAN, which averaged 1.5±1.6 mg N$_2$O m^{-2} day^{-1}. The higher rainfall around the MAN site could explain the higher N$_2$O emissions, as a result of increased soil moisture accelerating microbial nitrification and denitrification processes. For fluxes from the coast to SAN seasonality is present for all years, with high fluxes in the months of March through May, and in November through December. The first peak of N$_2$O flux is strongly associated with the wet season. The second peak of high N$_2$O flux recorded at SAN occurs during the dry season and can not be easily explained. However, about half of the dry season profiles exhibit significant correlations with CO, indicating a larger than expected source of N$_2$O from biomass burning. The average CO:N$_2$O ratio for all profiles sampled during the dry season is 94±77 mol CO:mol N$_2$O and suggests a larger biomass burning contribution to the global N$_2$O budget than previously reported.

1 Introduction

Nitrous oxide (N$_2$O) is the third most important anthropogenic greenhouse gas with a global warming potential about 310 times higher than CO$_2$ over a 100-year time-horizon. Currently, its radiative forcing is about 10% that of CO$_2$ (Hofmann, 2006). Its atmospheric lifetime is estimated to be 120 years (Schindlbacher, et al., 2004; IPCC, 2007). It also contributes to stratospheric ozone depletion (Cicerone, 1989). The most important N$_2$O sink (90%) is photodissocation above 30 km, with reaction with excited oxygen (10%) accounting for the balance. The atmospheric N$_2$O mixing ratio has been increasing from 270 ppb in 1750 to about 321 ppb in 2007, an increase of 19% (Fluckiger et al., 2002). The average annual growth rate from 1999 to 2000 was 0.85±1.1 ppb yr^{-1} (IPCC, 2007) and 0.73±0.06 ppb yr^{-1} from 1988–2005 (Hirsch, et al., 2006). The main reason is the increase in anthropogenic sources, like land use (N-fertilization) and industry, and current estimates are that about 40% of total N$_2$O emissions are anthropogenic (IPCC, 2007). The IPCC Fourth Assessment report (AR4) estimates 60% of total N$_2$O anthropogenic contribution (6.7 Tg N yr^{-1}) is from agricultural soils (1.7 to 4.8 Tg N yr^{-1}). Others authors have published that direct N$_2$O emissions from agricultural soils contribute about 77% of total anthropogenic contribution, with 6.2 Tg N yr^{-1} (Prather and Ehhalt, 2001;

Del Grosso et al., 2005; Hirsch et al., 2006) of $8.0\,\mathrm{Tg\,N\,yr^{-1}}$ (Kroeze et al., 1999; Hirsch et al., 2006).

Globally, the main sources of N_2O are nitrification and denitrification in soils ($6.6\,\mathrm{Tg\,N\,yr^{-1}}$) and the ocean ($3.8\,\mathrm{Tg\,N\,yr^{-1}}$) (IPCC, 2007; Flückiger, et al., 2002). About two thirds of the soil emissions occur in the tropics and approximately 20% are though to originate in wet rainforest ecosystems (Van Haren et al., 2005; Keller et al., 1993; Melillo et al., 2001). Other sources include gas-phase oxidation of NH_3, and industrial sources such as adipic acid and nitric acid production ($0.7\,\mathrm{Tg\,N\,yr^{-1}}$) and biomass burning ($0.7\,\mathrm{Tg\,N\,yr^{-1}}$) (Thiemens and Troggler 1991; IPCC, 2007). In tropical land, the main sources are likely to be natural soils with $3.3\,\mathrm{Tg\,N\,yr^{-1}}$ to $9.0\,\mathrm{Tg\,N\,yr^{-1}}$ (IPCC, 2007) ($16.4\,\mathrm{Tg\,N\,yr^{-1}}$ for Chapuis-Lardy, et al., 2007), followed by agricultural soils with $1.7\,\mathrm{Tg\,N\,yr^{-1}}$ to $4.8\,\mathrm{Tg\,N\,yr^{-1}}$ (IPCC, 2007) ($4.2\,\mathrm{Tg\,N\,yr^{-1}}$ for Chapuis-Lardy, et al., 2007), which are in agreement with other studies that suggest rain forests emit a large amount of N_2O (Keller et al., 1993, Melillo et al., 2001). Many studies in tropical forests, like the Amazon forest (Borchert, 1998; Jipp et al., 1998), agree that the average N_2O flux in these forests is much greater in the wet than dry season (Van Haren et al., 2005; Verchot et al., 1999; Perez et al., 2000; Garcia-Montiel et al., 2003; Wick, et al., 2005; Kiese et al., 2003). The soil source strength for N_2O is determined by the availability of substrates and the activity of nitrifying/denitrifying microbial communities, and on soil diffusivity, which is controlled mainly by soil water (Neftel et al., 2000; Smith et al., 2003), and on concurrent N_2O consumption process (Cavigelli and Robertson, 2001). Soil moisture conditions (Wick et al., 2005), temperature and pH (Huang et al., 2004; Wick et al., 2005) are some parameters that affect the rate of N_2O emission, naturally or in agricultural systems (Maggioto et al., 2000).

Studies in three different agricultural treatments in central Rondônia, Brazil, reported emissions ranging from -11.3 to $324.3\,\mathrm{mg\,N_2O\,m^{-2}\,day^{-1}}$ (Passianoto et al., 2003). Globally, Mosier et al. (1998) estimated emissions of $8.5\,\mathrm{Tg\,N\,yr^{-1}}$ for agricultural soils.

Many authors have also reported N_2O uptake by soil, although some have attributed the uptake to measurement uncertainty and have dismissed those results (Chapuis-Lardy et al., 2007; Donoso et al., 1990). However, other studies considered N_2O consumption by denitrifiers under high soil water contents and low soil temperature (Ryden, 1981; Glatzel and Stahr, 2001), low soil NO_3^- and N concentration (Rosenkranz et al., 2005), low pH (Knowles, 1982), and other factors. Others studies observed different conditions for N_2O soil uptake, such as high temperature (Yamulki et al., 1995) or high pH (Bremner and Blackmer, 1980), for example. This N_2O soil uptake could have important repercussions for quantifying the global source and the atmospheric lifetime of N_2O.

Studies in Amazonian forests have shown that primary forests emit significantly more N_2O than a pasture or un-
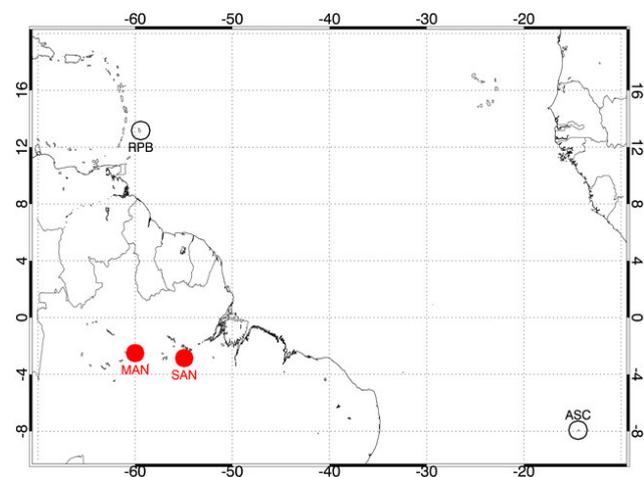
Fig. 1. Map of sampling sites used in this study. Open circles are marine boundary layer (MBL) background sites and filled circles are vertical profile sites within Brazil.

fertilized agriculture area (Do Carmo et al., 2005; Garcia-Montiel et al., 2003; Wick, et al., 2005; Verchot et al., 1999). However, do Carmo et al. (2005) observed that N treatments of pasture soils emitted about 10 times more N_2O than primary forest.

The work presented here involves aircraft vertical profiles of N_2O from 305 m to about 4 km (a.s.l.), over two sites in the Eastern and Central Amazon: Tapajós National Forest, near Santarém in the state of Pará; and Cuieiras Biologic Reserve, near Manaus in the state of Amazonas (Fig. 1). N_2O measurements over this 4 km altitude range are sensitive to fluxes over a large upwind fetch because of the strong and persistent trade winds, which is most likely to be the region between the sites and the Atlantic coast. To our knowledge, these regional scale N_2O measurements in Amazônia are unique and represent a new approach to looking regional scale emissions. In addition to the inherent uncertainties of extrapolation of inventory or "bottom-up" flux estimates, the major difference between our "top-down" approach and extrapolation is that our regional measurements implicitly integrate over all possible sources and sinks. This means that our measurements can constrain the total flux of N_2O, but without necessarily revealing much information on what processes may have contributed to the total. We apply a column integration technique (Miller et al., 2007) to estimate total surface emissions of N_2O and compare these fluxes to previous top-down and bottom up estimates for Amazonia and the tropics.

2 Methods

Above Tapajós National Forest (site code SAN), around 70 km south of Santarém, Pará, (since December 2000) and Cuieiras Biological Reserve (site code MAN), around 50 km
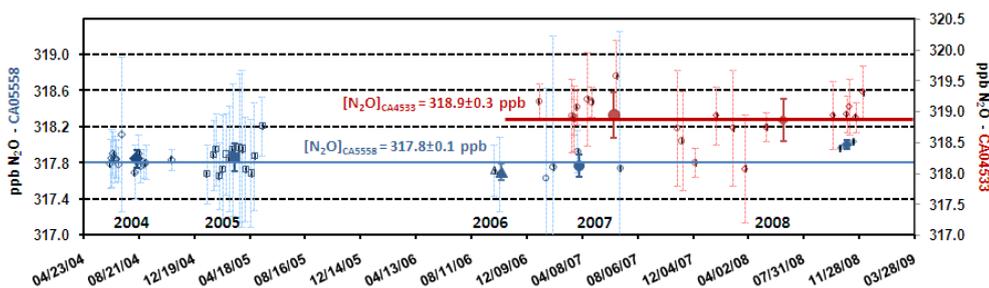
Fig. 2. N$_2$O times series for the tanks CA05558 (blue points) and CA04533 (red points). Each small point represents the mean of 20 aliquots for the tanks, and the error bars represent the one sigma standard deviation of the 20 analyses (repeatability). The large filled symbols represent the mean of all analyses for a given calendar year. The stability of the blue points, especially, demonstrates the long-term stability and precision of our system (reproducibility).

north of Manaus, Amazonas (since December 2004), air samples have been collected with semi-automatic portable sampling systems consisting of a portable flask package (PFP) which is shipped between the field site and laboratory and a portable compressor package (PCP), which remains at the site. The PFP contains 17 glass flasks with automated stopcocks and a logic controller board, and the PCP contains two pumps and batteries to power both the PCP and PFP. Each unit is contained within an aluminum suitcase. These two units are loaded into a light aircraft and a sampling inlet is stuck out of either the pilot window (MAN) or a wing vent (SAN) to connect the compressor unit to external air. To collect samples, the pilot uses a wired remote control allowing him to sample at pre-determined altitudes. The flights between 2000 and 2005 consisted of one descending and one ascending spiral vertical profile from 3660 m to 305 m and 305 m to 3600 m, over two locations separated by 30–100 km. Profiles obtained since 2006 are only descending from 4270 m to 305 m over just a single location for both sites, allowing for better vertical sampling resolution. Almost all profiles were sampled between 12:00–14:00 h LT (or near this time), because this is the time when the boundary layer is close to fully developed. The time variation between the ascending and descending profiles was about 30 min. So there is very small possibility of the wind direction change. From 2000 to 2003, flasks units with samples collected in Brazil were sent to the NOAA/ESRL laboratory in Boulder, CO USA, where they were analyzed for CO$_2$, CH$_4$, N$_2$O, SF$_6$, CO and H$_2$. Since 2004, a replica of NOAA analysis system for those gases has been operating at Instituto de Pesquisas Energéticas e Nucleares (IPEN) in São Paulo, SP Brazil. This analytical system is the Multiple Analysis of Gases Climate Change (MAGICC).

As the analytical system has not been previously described, we do so here. The N$_2$O and SF$_6$ analysis system is an ECD (Electron Capture Detector) chromatograph (HP 6890 Plus + model) with pre-column of 6 ft, 3/16″ o.d. 100/120 mesh Haysep Q and a column of 6 ft, 3/16″ o.d. 100/120 mesh Haysep Q and a 15 ml volume sample loop.

This system also uses a 10 port valve to inject the sample loop to pre-column, then just after the N$_2$O and SF$_6$ gas arrive to the column, the 10 port valve turns and starts a back flush in the pre-column to remove other gases. The carrier gas used in this system is an Argon/CH$_4$ (5% of CH$_4$) mixture.

MAGICC/IPEN has a mean repeatability for N$_2$O of 0.1 ppb (Fig. 2) as determined from the standard deviation of 20 consecutive aliquots from a high pressure cylinder of ambient air, which is very similar to that obtained at the NOAA lab (0.2 ppb). MAGICC/IPEN stability and precision was calculated analyzing the prepared tank CA05558 (blue in Fig. 2) which was analyzed periodically since 2004 and each time, we analyzed 20 aliquots. The variation of the means of the analyses in a given day is the repeatability. Since 2007 we added the periodic analyses of another tank calibrated at NOAA, CA04533 (red in Fig. 2). We also used this CA04533 tank to make an inter-comparison between the two laboratories (NOAA/ESRL and IPEN – Atmospheric Chemistry Laboratory (LQA)). The mean value of calibration at IPEN was 318.9±0.3 ppb N$_2$O and the calibration at NOAA was 318.8±0.2 ppb N$_2$O. This inter-comparison provides important evidence that after 2003, when the replica analysis system started makes the analysis, there is only a small artifact associated with this change. The standard gases used in the analysis are prepared by NOAA, and the inter-comparison program is continuous. In addition to our sites in Brazil, we used measurements on air samples collected at Ascension Island (ASC 7°55′ S, 14°25′ W) and Barbados, Caribbean (RPB 13°12′ N, 59°24′ W) as part of the NOAA Earth System Research Laboratory (NOAA/ESRL) global air sampling network. This air was sampled into 2.5 l glass flasks with Teflon-tipped glass stopcocks and filled to about 1.2 bar (Conway et al., 1994), and shipped to NOAA for analysis to laboratory.

At SAN, the ascending profiles were made above the Tapajós National Forest (02°51′ S, 54°58′ W), near the "km 67" tower that is located around 7 km to the east of the Tapajós river. Descending profiles were made 30 km to
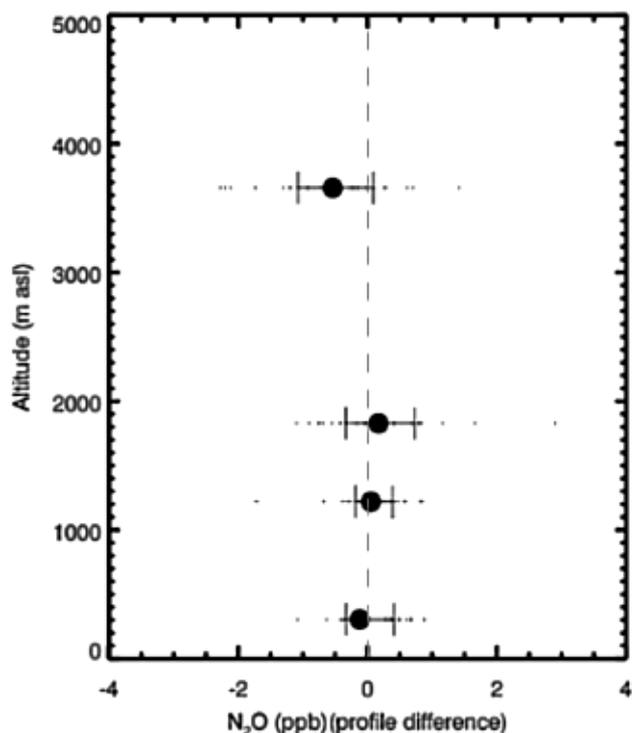
Fig. 3. Differences between ascending and descending profiles at SAN. The error bars show the 25th and 75th percentiles of the differences between the profiles at SAN. The small dots are the individual differences. The median values (50th percentiles) are the large symbols.

Fig. 4. N$_2$O Time Series, Marine boundary layer sites ASC, RPB (thin lines) and FTL, above of 1500 m and below of 1200 m for **(a)** SAN and **(b)** MAN vertical profile average.

the east of the tower, above an agriculturally impacted area (02°52′ S; 54°41′ W), in order to assess the impact of possible local influences. At MAN, descending profiles were made above the "K34" eddy covariance tower at Cuieiras Biological Reserve (2°35′ S, 60°12′ W) 50 km north of Manaus (population 1.8 million), and ascending profiles were made 100 km east (typically upwind) of the tower, above undeveloped forest (2°30′ S, 59°05′ W). 20km east from tower, i.e., between the 2 sites, there is the road and farmers. The comparison between preserved area and tower site was made to assess possible influence of farms, transport and the city of Manaus.

At both sites, differences between ascending and descending profiles were generally small compared to differences with the marine background, showing that local influence relative to that between the sites and the coast was negligible (Fig. 3). In order to sample the vertical structure of the background air entering the Amazon basin, between 2000 and 2003, several vertical profiles were collected 50 km northeast of Fortaleza, state of Ceará (site code FTL 4°09′ S, 38°16′ W), in the Atlantic coast of Brazil (Fig. 1).

3 Results

In order to analyze the N$_2$O time series (Fig. 4), it is necessary define a background N$_2$O mixing ratio representing the air entering Brazil off the Atlantic Ocean. This helps to remove the global and tropical trends that influence N$_2$O within the Amazon basin. Air entering the Amazon basin is dominated by trade-wind easterlies coming from the tropical Atlantic Ocean, with relative influence of Northern and Southern Hemisphere air which depends upon the seasonally varying latitude of the Inter-Tropical Convergence Zone (ITCZ). Considering this seasonality, two NOAA monitoring sites were chosen to represent air from each hemisphere: RPB and ASC. Between 2000 and 2003, 10 vertical profiles over FTL were also collected. A comparison of these flights with the RPB and ASC time series shows that FTL is bounded by ASC and RPB, confirming that air from both hemispheres influence the Amazon basin background. Additionally, FTL data shows minimal vertical gradients in N$_2$O validating our assumption that marine boundary layer data
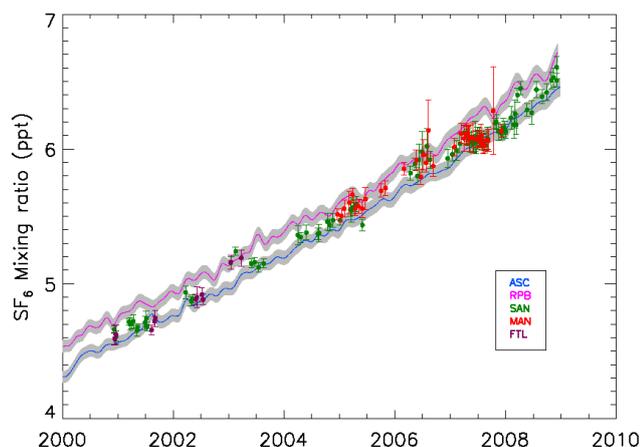
Fig. 5. SF$_6$ Time Series. Marine boundary layer sites ASC, RPB (thin lines); FTL, MAN and SAN vertical profiles means.

can be used to represent the column of air entering the continent.

The profiles show the integrated impact of N$_2$O surface emissions for the areas between the Atlantic coast and the sampling sites. Analyzing Fig. 4, we observe that before 2004 the eastern Amazon N$_2$O mixing ratio was generally between that of the two background sites, indicating only modest additions to the zonal background from Amazonian fluxes. However, since 2004 N$_2$O mixing ratios over SAN and MAN were higher than background by 0.7 and 1.0 ppb, on average, respectively. Notably, this is significantly higher than 0.1 ppb, which is the difference of calibration between NOAA and IPEN, indicating that the observed difference can not be explained by the analysis laboratory change. The largest enhancements are in the convective boundary layer (CBL; which we define here for illustrative purposes as altitudes less than 1200 m asl), although there are noticeable enhancements in the free troposphere, possibly indicating the convective redistribution of N$_2$O emitted into the CBL. The higher N$_2$O mixing ratios in the CBL indicate surface flux of N$_2$O by these two regions in Amazonia. The differences between our SAN or MAN measurements and the Atlantic background can be used to quantify N$_2$O fluxes.

Because of strong convection one cannot count on surface emissions to be trapped in the CBL, so we use a column integration technique (Miller et al., 2007) that does not distinguish the CBL and free troposphere. To apply the column integration technique, we estimate the background N$_2$O mixing ratio representing the air entering Brazil off the Atlantic Ocean using sulfur hexafluoride (SF$_6$, a purely anthropogenic gas) as a transport tracer, because the relative Northern and Southern Hemisphere contributions to the N$_2$O background vary and depend on the seasonally varying latitude of the ITCZ. SF$_6$ has no regional sources or sinks in Amazon basin (Olivier, 1999), so we consider the SF$_6$ mixing ratio in the Amazon Basin as the same as that of the air entering

Brazil. Figure 5 shows that the vast majority of the time SF$_6$ at SAN and MAN is bounded by the time series from ASC and RPB. Using a simple two-end-member mixing model, we then calculate the fractions of air arriving at our Amazonian sites that can be represented by the background sites ASC and RPB, and can then be applied to any other conserved tracer (Eqs. 1 and 2) (Miller et al., 2007).

$$\text{ASC}_{(\text{SITE})} = 1 - \text{RPB}_{(\text{SITE})} = \frac{\text{SF}_{6(\text{SITE})} - \text{SF}_{6(\text{RPB})}}{\text{SF}_{6(\text{ASC})} - \text{SF}_{6(\text{RPB})}} \quad (1)$$

$$X_{\text{bg}} = \text{ASC}_{\text{SITE}} \cdot X_{\text{ASC}} + \text{RPB}_{\text{SITE}} \cdot X_{\text{RPB}} \quad (2)$$

ASC$_{(\text{SITE})}$ and RPB$_{(\text{SITE})}$ represents the ASC and RPB fraction, respectively, for a specific site; SF$_{6(\text{SITE})}$ represents the SF$_6$ mixing ratio for each specific site (SAN or MAN), and SF$_{6\text{ASC or RPB}}$, is the SF$_6$ mixing ratio at ASC and RPB, respectively. X$_{\text{bg}}$ represents the background mole fraction of the gas (N$_2$O in this case) for a specific site (SAN or MAN); and X$_{\text{ASC or RPB}}$ is the mixing ratio at ASC or RPB. Note that we do not bound the values of ASC$_{\text{site}}$ between 0 and 1, which assumes that the SF$_6$ and N$_2$O gradients between ASC and RPB extend further north and south beyond the background sites. Figure 6 presents four example original and "corrected" N$_2$O vertical profiles in different years for SAN and MAN to illustrate the SF$_6$-based background subtraction process.

We calculated the N$_2$O flux from the eastern Amazon basin by integrating the N$_2$O mixing ratio difference (coast to sample site) shown in Fig. 6b from the surface to the top of the profile according to Eq. (3) (Miller et al., 2007) for each profile. This flux represents the flux contribution from the coast to the sample site.

$$F_{\text{N}_2\text{O}} = \frac{\int_{z_i}^{z_f} [(X_{\text{N}_2\text{O}})_{\text{SITE}} - (X_{\text{N}_2\text{O}})_{\text{bg}}]dz}{t} \quad (3)$$

Here, X$_{\text{N}_2\text{O}}$ is the concentration in units of mol m^{-3}, which can be determined from mole fraction observations and estimated vertical profiles of temperature and pressure. z_i and z_f are the minimum and maximum range of vertical integration that is defined between altitudes of profile, ground level ($\sim$300 m) to the top of the profile ($\sim$4 km). t was determined for each altitude, counting the time (in days) the air took to travel between the coast and the sampling site in the back trajectory simulated by the Hysplit model (Fig. 7) (Draxler, 2003 – www.arl.noaa.gov/ready/open/hysplit4.html), which uses FNL winds from the NCEP global model. Note that when a back trajectory reached low altitudes ($<$50 m a.g.l.) before the coast, or in other instances where trajectories could not be calculated, a default value of 2 days was used for t. This is an improvement over the approach of Miller et al (2007), who used a constant value for t of 2$\pm$1 days. However, sensitivity tests for both CH$_4$ and N$_2$O showed that using a nominal value of 2 days did
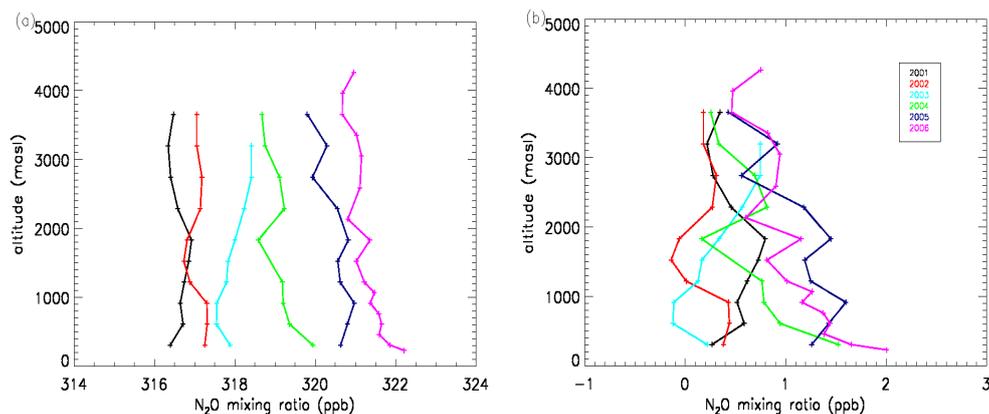
Fig. 6. Six sample N₂O vertical profiles for different years (2001–2006): **(a)** raw data and **(b)** with background subtracted, thus removing the global and/or regional trends.
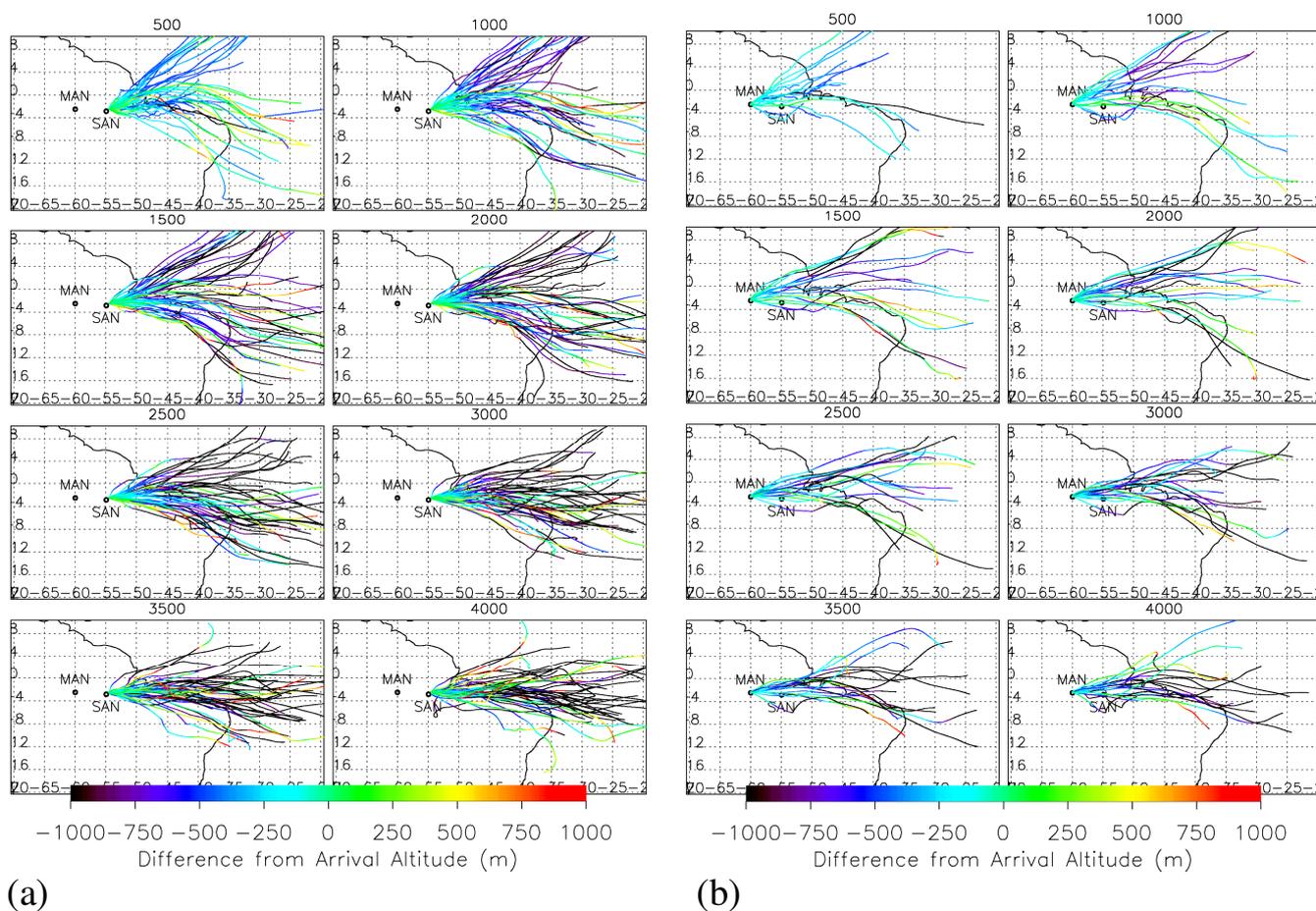
Fig. 7. Back trajectories for **(a)** SAN and **(b)** MAN for altitudes from 500 to 4000 m each 500 m, used to estimate the time t which air masses took to travel from the coast to the sampling site, obtained with Hysplit back-trajectory model (Draxler, 2003 – www.arl.noaa.gov/ready/open/hysplit4.html.) used to calculate N₂O flux. The colorbar represents the difference from the arrival altitude (shown as the title of the plot) at any point along the trajectory.

not significantly affect the annual or seasonal flux averages. The back trajectory simulated by Hysplit model confirms for both sites the initial statement and the SF$_6$ observations that air from both Hemispheres enters the basin. Air arriving at the sites above 3000 m appears to originate from a narrower north-south band centered on the equator.

Uncertainty in SF$_6$ and N$_2$O values at ASC and RPB used in Eqs. (1) and (2) are 0.05 ppt and 0.34 ppb respectively, based on the scatter about smooth curve fits in Fig. 4 (shown by the gray error band). Uncertainty in $(X_{N2O})_{site}$ in Eq. (3) is the measurement uncertainty of 0.2 ppb and $(X_{N2O})_{bg}$ is 0.26 ppb, as determined by propagating uncertainties through Eqs. (1) and (2). The F_{N2O} uncertainty is estimated by propagating uncertainty from all term in Eqs. (1–3) and is typically 0.72 mg N$_2$O m^{-2} day^{-1}. There is a small source of N$_2$O in the atmosphere that comes from oxidation of NH$_3$, which is estimated to be ∼0.6 Tg N/yr globally, with most coming from agricultural and industrial sources. In comparison, tropical forest soils are typically estimated to be an order of magnitude larger. Neglecting this source could potentially give a high bias to our surface flux estimates as large as 5–10% at most.

Our analysis requires combining measurements from two labs; therefore calibration as well as comparison of actual samples become very important. We made two kinds of comparisons between the IPEN and NOAA laboratories, and sensitivity tests were made in order to examine possible bias between NOAA and IPEN. In addition to the tank comparison mentioned above, which showed a difference of 0.1±0.3 ppb, another comparison was made by analyzing flasks sampled at the Arembepe site (site code ABP 12°58′ S, 38°30′ W) in 2008. In the same day, two flasks were sampled for NOAA and two sampled for IPEN with a difference of 20–40 min between them. This comparison shows a bias between IPEN and NOAA of 0.3±0.5 ppb, in average. This comparison is significantly noisier than the tank inter-comparison as seen by the 0.5 ppb uncertainty in the difference. The period used in this comparison corresponds to 2008, due to likely sampling problems in 2006 and 2007 at Arembepe. To test the impact of a possible measurement bias on our analysis, after 2004 we subtracted 0.3 ppb from the IPEN measurements and recalculated the fluxes. As expected, the mean fluxes were smaller, but the ratios between seasons and sites were not strongly affected, as shown in Table 1.

The fluxes calculated from all profiles from the coast to SAN or MAN are plotted in Fig. 8, *a* and *b* respectively. The flux climatology exhibits significant seasonality for SAN. There are two times of the year that show high fluxes: March until May, and November and December. For fluxes from coast to MAN, the seasonality is less pronounced with the maximum emissions centered on April. However, the annual mean flux between the coast and MAN is 2.1±1.0 mg N$_2$O m^{-2} day^{-1}, which is higher than that for the coast to SAN, which is 1.6±1.4 mg N$_2$O m^{-2} day^{-1}. The standard deviation of fluxes (1.0 and 1.4 mg N$_2$O m^{-2} day^{-1}) is
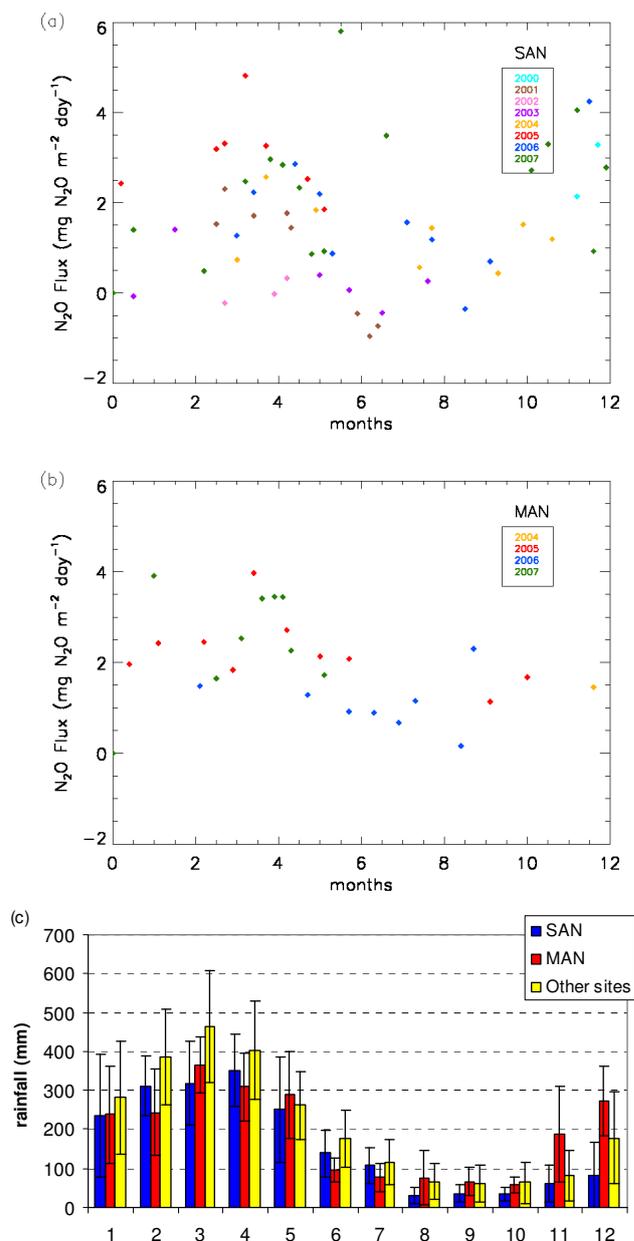
Fig. 8. N$_2$O Fluxes upwind of **(a)** SAN between 2000 and 2007 and **(b)** MAN between 2004 and 2007. **(c)** Average rainfall for SAN (blue), MAN (red) and seven sites (yellow) located upwind of the sample sites: Belém, Breves, Cametá, Itacoatiara, Porto de Moz, Souré, Tucuruí (INMET – http://www.inmet.gov.br). The averages were calculated using data between 2001 and 2007 for SAN and "Other sites" and 2004 to 2007 for MAN. The error bars represent the standard deviation across years.

substantially larger than the uncertainty for a single profile (∼0.7 mg N$_2$O m^{-2} day^{-1}). This suggests that the seasonal and interannual variability is largely geophysical and not simply a result of the calculation uncertainty. Although the mean value for MAN is higher, the flux variability for SAN

Table 1. Sensitivity of the possible bias between NOAA and IPEN labs.

Flux (mg N$_2$O m^{-2} day^{-1})	SAN WET	SAN DRY	MAN WET	MAN DRY
Original	1.45±1.4	1.72±1.4	2.53±0.9	1.56±0.8
Original − 0.3 ppb	0.94±1.2	1.13±1.1	1.68±0.8	1.10±1.0
difference	0.51±2.6	0.59±2.5	0.85±1.5	0.46±1.8
	In space (SAN/MAN)		Over time (WET/DRY)	
			SAN	MAN
Original	1.01		1.18	1.65
Original − 0.3 ppb	1.23		1.46	1.93
difference	18%		19%	14%

is higher, which reflects the greater seasonality of fluxes upwind of SAN. The higher seasonal flux variability seen at SAN most likely reflects the stronger seasonality in precipitation seen in eastern Amazonia (Fig. 8c).

Soil emission is the most important contribution to N$_2$O flux (6.6 Tg N yr^{-1}) (IPCC, 2007) and occurs by activity of nitrifying/denitrifying microbial communities in soil (Chapuis-Lardy, et al., 2007; Davidson et al., 2004; Garcia-Montiel et al., 2003; Passianoto et al., 2003). In some regions of Amazon basin, an additional contribution could be agricultural processes (2.8 Tg N yr^{-1} globally) (IPCC, 2007), mainly in Pará, where significant forest conversion has occurred over the past 10 years. The direct ocean influence was removed when the background was subtracted, and is expected to be significantly smaller than soil or agricultural emissions. Both the soil emission and agricultural sources can be influenced by soil water and thus precipitation. To see if precipitation could explain the seasonal flux patterns inferred from the MAN and SAN observations, we calculated monthly mean precipitation for a) SAN b) MAN and c) the average of seven sites (Belém, Breves, Cametá, Itacoatiara, Porto de Moz, Souré, Tucuruí) upwind of SAN and MAN (Fig. 8c). All rainfall data were obtained from Instituto Nacional de Meteorologia (INMET: www.inmet.gov.br) and were composed of station data from 2001–2007.

Comparing fluxes and rainfall (Fig. 8) it is evident that the first peak of N$_2$O flux at SAN appears strongly related to wet season precipitation. The flux peak derived from MAN data also corresponds to high rainfall. Furthermore, the higher rainfall in Amazonas, even during the dry season (August to December), could contribute to the high value of N$_2$O emission that persists throughout the year. Plot-scale studies have also observed a strong relationship between precipitation and N$_2$O flux (e.g., Cattannio et al., 2002; Do Carmo et al., 2005).

We studied the fluxes classifying them by season (Fig. 9). For SAN we classified fluxes into wet (W), transition wet to dry (W/D) and dry (D) seasons. For MAN we separated fluxes only into wet and dry seasons. All the classifications were made based on local precipitation (Fig. 8c). For SAN
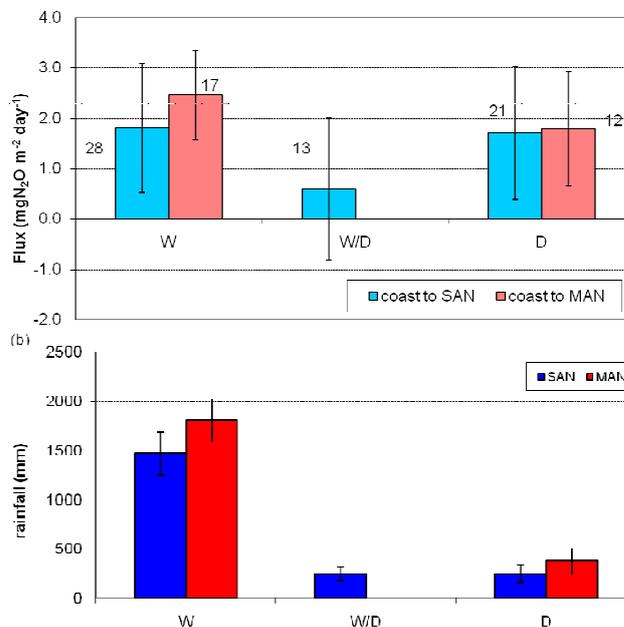
Fig. 9. Trimester (three-month) average **(a)** N$_2$O fluxes from coast to SAN and MAN for all studied years, **(b)** rainfall for SAN (blue), MAN (red). The error bars represent the standard deviation of all fluxes and rainfall in Fig. 8 within each trimester, and the numbers represent the number of profiles for the same period for fluxes.

the months classification are: 1. W: January to May, 2. W/D: June and July, 3. D: August to December. In some years (as in January of 2003 and 2005) there was a delay in the beginning of wet season in January so that some profiles of this month were classified as dry season. For MAN the month classifications are: W: November to May, D: June to October. With this classification, we observe less variability in fluxes derived from MAN data than from SAN data. For fluxes based on SAN data, a strong seasonality is evident. In Fig. 8, we note the presence of negative fluxes, which we do not interpret as uptake signals, but most likely occur due

to incorrect specification of the background or other errors in our calculation method. Our simple model is sensitive to such errors and the fluxes calculated using Eq. (3) are best interpreted seasonally, as displayed in Fig. 9. For MAN data, no negative fluxes are calculated which probably reflects the high mean fluxes recorded there. From the coast to SAN, during the dry and wet seasons N$_2$O fluxes were similar but fluxes were lower during the transition season. From the coast to MAN, during the wet season N$_2$O fluxes were higher than during the dry season, with a more gradual transition to the dry season than seen at SAN. Comparing fluxes derived from observations at each site, during the wet season, fluxes derived from MAN are almost 0.5 mg N$_2$O m^{-2} day^{-1} higher than those at SAN. This behavior is very different during dry season, when both places exhibit similar fluxes. From the coast to SAN, we expected the same dry season behavior observed from coast to MAN, i.e., decrease of fluxes relative to the wet season. The high N$_2$O flux during the dry season over the trajectories from the coast to SAN suggests the presence of a source other than soil emissions. Back trajectories in Fig. 7 show that air arriving at MAN tends to be from the east and northeast, whereas air arriving at SAN tends to be from the east and southeast. Areas east and southeast of SAN are more agriculturally developed than areas northeast of MAN which are more heavily forested. This difference in landscape could be related to the different seasonal patterns and absolute amounts of N$_2$O flux derived from the measurements at each site.

In addition to seasonal variability, we also observe substantial interannual variability in the fluxes recorded at SAN. For example, our observations indicate lower than average fluxes in 2002, which is consistent with the plot-scale observations of Davidson et al (2004) that showed a decrease of more than 50% in 2002 compared to the wet seasons of 2000 and 2001. In contrast, fluxes from 2005 were much higher than average. There is only a weak relationship ($r^2 = 0.22$) between year to year variations in precipitation (as measured at Santarem) and upwind N$_2$O emissions. Regardless of the cause of the variations, the large degree of variability in both seasonal and interannual fluxes emphasizes the necessity of long-term monitoring of atmospheric N$_2$O in Amazonia.

Another important N$_2$O source could be biomass burning, which at the global scale is estimated to account for only 4% of all emissions (IPCC, 2007). We compared N$_2$O and CO vertical profiles in order to see if biomass burning might be a significant contributor to dry season N$_2$O fluxes recorded at SAN. CO has been used as an atmospheric tracer of biomass burning at a variety of scales (e.g., Langenfelds et al., 2002; Gerbig et al., 2003; van der Werf et al., 2004). A commonly used compilation of emission ratios (Andreae and Merlet, 2001) gives a best guess biomass burning emission ratio for tropical forests of 817 mol CO/mol N$_2$O. This suggests very little N$_2$O is emitted from fires as in the global budgets. However, in some of our vertical profiles we found evidence for a significant relationship between N$_2$O and CO
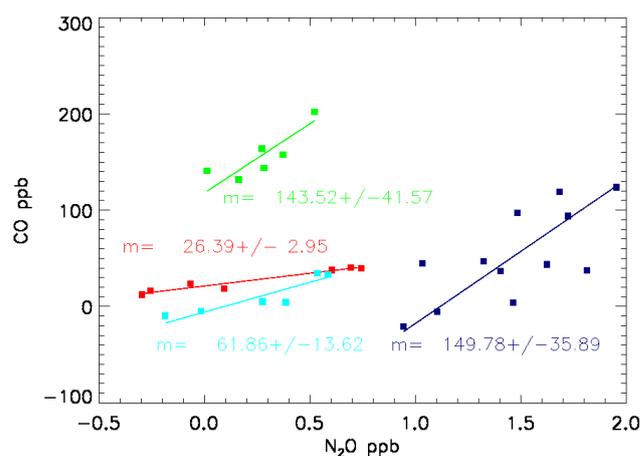
Fig. 10. The 6 higher descendant CO/N$_2$O ratios obtained for the profiles. The y equation represents the line equation for the points and R^2, the dependence between the variables (CO and N$_2$O).

in the dry season (Fig. 10). From the total of 25 profiles sampled during the SAN dry season, 28% (7 profiles) exhibited correlations (r^2) higher than 0.5 and a mean ratio of 99.0±89.8 mol CO/mol N$_2$O, nearly an order of magnitude larger than Andreae and Merlet (2001). 44% (11 profiles) exhibited correlations higher than 0.3 with a mean ratio of 100.6±68.9 mol CO:mol N$_2$O. All correlations higher than 0.3 were statistically significant at $p < 0.05$ (using a two-tailed t-test). The average ratio of all 25 profiles during the dry season, is 93.8±76.6 mol CO:mol N$_2$O. However, poor or negative correlations between CO and N$_2$O were also observed in the dry season, indicating that dry season emissions other than biomass burning may also be required to explain our dry season flux maximum observed at SAN. As a rough estimate of the global N$_2$O emissions from biomass burning, consistent with our observed ratios, we scale N$_2$O biomass burning emissions to those of CO. Taking a global biomass burning estimate of 3.53 P C yr^{-1} (van der Werf et al., 2004) and an average CO:C molar emission ratio of 0.075 (Andreae and Merlet, 2001), we estimate global CO emissions from biomass burning of 618 Tg CO yr^{-1}. Given our average of about 100 mol mol^{-1} for CO:N$_2$O, we estimate N$_2$O biomass burning emissions of 6.2 Tg N yr^{-1} assuming that tropical emission ratios for N$_2$O and CO are similar to the global flux-weighted average, which is reasonable considering that most biomass burning is tropical. Our results suggest that biomass burning emissions of N$_2$O may be a significantly larger contributor to the tropical and global N$_2$O budgets than previously thought, although more investigation on this needed.

We interpret our flux results to be representative of large regions, namely the $\sim 10^5$–10^6 km^2 area between the sites and the Atlantic coast. If our fluxes were in fact more locally representative, then we would expect the lowest altitudes measured to contain the majority of the signal. In order

Table 2. Comparison of N_2O fluxes in global, regional and plot scale at Amazon Brazilian Basin.

Ecosystem/Location	Period	Season	Flux ($mg\,N_2O\,m^{-2}\,day^{-1}$)
Global-scale			
GEIA tropical land[1]	1990	Annual	0.95
Hirsch et al. tropical land[1]	1998–2001	Annual	1.54±0.55
GEIA South America[1]	1990	Annual	1.55
Hirsch et al. South America[1]	1998–2001	Annual	2.50±0.89
Hirsch et al.South America [1]	2002–2005	Annual	1.6±0.5
Regional-scale			
Coast to SAN[2]	2001–2007	Wet	1.42±1.62
Coast to SAN[2]	2001–2007	Dry	1.62±1.69
Coast to MAN[2]	2004–2007	Wet	2.73±1.15
Coast to MAN[2]	2004–2007	Dry	1.94±1.56
Plot-scale			
PF Porto Velho, RO[3]	1992–1999	Wet; Dry	(1.5±0.4); (2.3±0.4)
PF Jamari, RO[3]	1992–1999	Wet; Dry	(3.4±1.0); (1.6±0.4)
PF Caucalândia, RO[3]	1992–1999	Wet; Dry	(2.6±0.4); (2.5±0.4)
PF Novo Vida, RO[3]	1992–1999	Wet; Dry	(1.9±0.4); (1.3±0.3)
PF Ouro Preto, RO[3]	1992–1999	Wet; Dry	(4.1±1.8); (1.8±0.2)
PF Manaus, AM[4]	1992–1999	Annual	0.4
PF SAN, PA[5a]	2001–2002	Annual	1.3±0.2
PF SAN, PA[5b]	2001–2002	Annual	2.2±0.9
PF SAN, PA[5c]	2000–2002	Wet; Dry	4±2; 1±0.5
PF Santarém, PA[6]	1999/2000	Annual	2.9–4.1
PF Nova Vida, RO[7]	2001	Annual	4.0±0.8
YP RO[4]	1992–1999	Annual	2.7–4.34
YP Nova Vida, RO[7]	2001	Annual	0.2±0.1
OP RO[4]	1992–1999	Annual	0.1–0.3
TA Nova Vida, RO[7]	2001	Annual	0.6±0.3

[1]Hirsch et al., 2006, average of scenarios A, B, C, D, G; S. American totals derived by scaling tropical land totals by ratio of tropical S. American to tropical land flux in GEIA. ; [2]This study; [3]Neil et al., 2005; [4]Coolman, 1994; [5]Davidson et al., 2004 [a] exclusion treatment, [b] control, wet and dry season from control treatment (uncertainty represents interannual variability); [6]Wick et al., 2005; [7]Do Carmo et al., 2007; [8]Stehfest and Müller, 2004. PF = Primary Forest; YP = Young Pasture; OP = Old Pasture; TA = Treatment Area

to test this, we conducted sensitivity tests to assess the influence of the lower altitudes on our flux calculations. We integrated the fluxes from the surface to 4270 m, but systematically excluded observations below a given height (152 m, 300 m, 600 m and 1000 m), thereby assuming the mole fraction at that given height was constant to the surface. The last altitude was chosen to represent the mid or upper CBL, and the first one (152 m) the control altitude representing the default integration. The variation between flux values from the four starting altitudes was less than 5%, which suggests a regional influence for our fluxes. In general, we also expect that our flux estimates are biased low, because the upper limit of our integral does not fully capture all convective redistribution of flux, which in the Amazon basin may extend all the way toward the tropopause near 15 km. However, based on the shapes of our observed profiles, which show distinct

differences between the CBL and free troposphere of 0.5 ppb N_2O, we do not expect that our flux estimates are significant underestimates.

One important way to interpret our fluxes is by comparing our regional flux values to plot-scale fluxes from Amazonian forest and pasture sites, and global-scale estimates (Table 2): both bottom-up (e.g. Bouwman, et al., 1995) and top-down (e.g. Hirsch et al., 2006; Huang et al., 2008) sources. In general, N_2O fluxes reported at a variety of scales show general agreement, despite significant variability in the fluxes. Comparing to plot-scale fluxes, differences can be expected as a result of the site-specific conditions for each plot-scale study. For example, looking just at the fluxes from the south-western Amazonian state of Rondonia (RO in Table 2), fluxes vary from 0.1 to 4.3 $mg\,N_2O\,m^{-2}\,day^{-1}$. The large site to site variability seen at the plot scale might also

help to explain the high variability of our fluxes, because our fluxes will be influenced to some extent by all ecosystems between the coast and the sample site. This is especially true in the case of SAN, where the upwind landscape is composed of undisturbed forest, pasture, fertilized agricultural land and to the southeast, some grassland. Thus, changes in wind or the behavior in any one of these ecosystems could significantly influence our observations. In addition to the annual fluxes, our regional flux results are also similar to the seasonality observed in plot-scale fluxes. The study of Davidson et al. (2004), in particular, shows a very strong N$_2$O flux response to moisture. This is the case both for the comparison of the throughfall exclusion and control areas and within the normal wet-dry transition within the control area. Neil et al. (2005) studied different forests in Rondônia. Although two of six primary forests studied showed the same (Cacaulandia) or higher (Porto Velho) N$_2$O fluxes in the dry season compared to wet, the overall pattern was still that of higher N$_2$O fluxes during the wet season. The fact that some plot-scale studies do show elevated dry season fluxes could help explain our observation of high dry season N$_2$O fluxes that are not correlated with high CO. In addition to the correlation between N$_2$O and CO during the dry season, we plotted CO fluxes (calculated in the same way as the N$_2$O fluxes) vs. N$_2$O fluxes for SAN and MAN (Fig. 11) for all profiles sampled during this season. We observed three kinds of correlation for upwind of SAN. First, there are a set of sampling days where a clear relationship between CO and N$_2$O fluxes exist. There are also days in which we see high N$_2$O with only moderate CO fluxes and also high CO fluxes, with small N$_2$O fluxes. The causes of N$_2$O dry season flux variability observed at SAN can not be explained by biomass burning alone, and our analysis suggests that a variety of processes are likely responsible for the variability. In contrast, for data from MAN we did not observe any correlation for CO and N$_2$O during dry season.

Our regional estimates are also consistent with large scale bottom-up and top-down estimates (Table 2). Our estimates based on MAN and SAN data are higher than the GEIA bottom-up estimates, but more similar to the top-down estimates of Hirsch et al (2006), who used marine boundary layer atmospheric N$_2$O data to optimize the GEIA fluxes using an inverse model. The correspondence of our regional flux estimates with the larger scale N$_2$O flux estimates confirms the importance of Amazonia in the global N$_2$O budget.

4   Conclusion

Considering the mean of the all studied years, the region between the coast and MAN presented higher N$_2$O fluxes (2.1±1.0 mg N$_2$O m^{-2} day^{-1}) than the region between the coast and SAN (1.5±1.6 mg N$_2$O m^{-2} day^{-1}), which is consistent with the higher rainfall upwind of MAN, including during the dry season (August to December). The seasonal
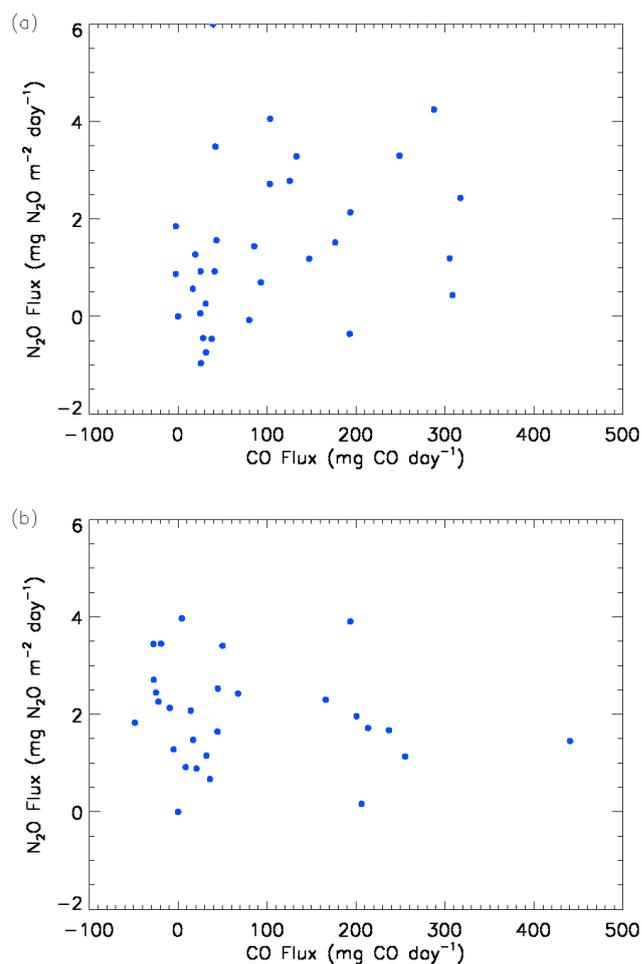
Fig. 11. Correlation between N$_2$O and CO fluxes during all dry seasons sampled for **(a)** SAN and **(b)** MAN. It is possible observe correlation just at up wind SAN fluxes.

and interannual variability present in our data suggests that long term measurements covering all seasons are required to understand the dynamics of N$_2$O emissions in Amazonia.

We calculated large seasonality in the fluxes from SAN for all years, with high fluxes in the months of March through May, and in November through December. Based on the recorded precipitation seasonality and previous plot scale studies the wet season N$_2$O emissions are likely dominated by forest soil emission accelerated by soil moisture. The unexpectedly high N$_2$O emission during the dry season, however, suggests a combination of biomass burning and other sources. The low emission ratios between CO and N$_2$O we observed averaging 94±77 ppbCO/ppbN$_2$O also suggest that at global scales the importance of biomass burning to the N$_2$O budget may be underestimated.

References

Andreae, M. O. and Merlet, P.: Emission of trace gases and aerosols from biomass burning, Global Biogeochem. Cy., 15(4), 955–966, 2001.

Borchert, R.: Responses of tropical trees to rainfall seasonality and its long-term changes, Clim. Change, 39, 381–393, 1998.

Bouwman, A. F., van der Hoek, K. W., and Olivier, J. G. J.: Uncertainties in the global source distribution of nitrous oxide, J. Geophys. Res., 100, 2785–2800, 1995.

Bremmer, J. M. and Blackman, A. M.: Mechanisms of nitrous oxide production in soils, In: Biochemistry of Ancient and Morden Environment, edited by: Trudinger, P. A., Walter, M. R., and Ralph, R. J., Australian Academy of Science, Canberra, Australia, 1980.

Cattannio, J. H., Davidson, E. A., and Nepstad, D. C.: Unexpected results of a pilot throughfall exclusion experiment on soil emissions of CO_2, CH_4, N_2O, and NO in eastern Amazonia, Biol. Fert. Soils, 36, 102–108, 2002.

Cavigelli, M. A. and Robertson, G. P.: Role of denitrifier diversity in rates of nitrous oxide consumption in a terrestrial ecosystem, Soil Biol. Biochem., 15, 531–536, 2001.

Chapuis-Lardy, L., Wrage, N., Metay, A., Chottes, J-L. and Bernouxs, M.: Soils, a sink for N_2O? A review, Global Change Biol., 13, 1-17, 2007.

Cicerone, R. J.: Analysis of sources and sinks of atmospheric nitrous-oxide (N_2O), J. Geophys. Res.-Atmos., 94(D15), 18265–18271, 1989.

Conway, T. J., Tans, P. P., Waterman, L. S., and Thoning, K. W.: Evidence for interannual variability of the carbon-cycle from the national-oceanic-and-atmospheric-administration climate-monitoring-and-diagnostics-laboratory global-air-sampling-network, J. Geophys. Res.-Atmos., 99(D11), 22831–22855, 1994.

Coolman, R. M.: Nitrous Oxide Emissions from Amazonian Ecosystems, Ph.D. dissertation, North Carolina State University, 1994.

Davidson, E. A., Ishida, F. Y. and Nepstad, D. C.: Effects of an experimental drought on soil emissions of carbon dioxide, methane, nitrous oxide, and nitric oxide in a moist tropical forest, Global Change Biol., 10, 2582–2590, 2004.

Del Grosso, S. J., Mosiera, A. R., Partonb, W. J., and Ojimab, D. S.: DAYCENT model analysis of past and contemporary soil N_2O and net greenhouse gas flux for major crops in the USA, Soil Till. Res., 83, 9–24, 2005.

Do Carmo, J. B., Andrade, C. A., Cerri, C. C., and Piccolo, M. C.: Nitrogen availability and N_2O fluxes from pasture soil after herbicide application, R. Bras. Ci. Solo, 29, 735–746, 2005.

Donoso, L., Santana, R. and Sanhueza, E.: Seasonal variation of N_2O fluxes at a tropical savannah site: soil consumption of N_2O

during the dry season, Geophys. Res. Lett., 20(13), 1379–1382, 1993.

Draxler, R. R. and Rolph, G. D.: HYSPLIT (HYbrid Single-Particle Lagrangian Integrated Trajectory) Model access via NOAA ARL READY Website (http://www.arl.noaa.gov/ready/hysplit4.html), NOAA Air Resources Laboratory, Silver Spring, MD, USA, 2003.

Flückiger, J., Monnin, E., Stauffer, B., Schwander, J., and Stocker, T.F.: High-resolution Hlocene N_2O ice core record and its relationship with CH_4 and CO_2, Global Biogeochem. Cy., 16(1),1010, 2002.

Garcia-Montiel, D., Steudler, P. A., Piccolo, M., Neill, C., Melillo, J., and Cerri, C. C.: Nitrogen oxide emissions following wetting of dry soils in forest pastures in Rondônia, Brazil, Biogeochem. J., 64, 319–336, 2003.

Gerbig, C., Lin, J. C., Wofsy, S. C., Daube, B. C., Andrews, A. E., Stephens, B. B., Bakwin, P. S. and Grainger C. A.: Toward constraining regional-scale fluxes of CO_2 with atmospheric observations over a continent: 2. Analysis of COBRA data using a receptor-oriented framework, J. Geophys. Res., 108(D24), 4757, doi:10.1029/2003JD003770, 2004.

Glatzel, S. and Stahr, K.: Methane and nitrous oxide exchange in differently fertilized grassland in southern Germany, Plant Soil, 231, 21–35, 2001.

Hirsch, A. I., Michalak, A. M., Bruhwiler, L. M., Peters, W., Dlugokencky, E. J., and Tans, P. P.: Inverse modeling estimates of the global nitrous oxide flux from 1998-2001, Global Biogeochem. Cy., 20, GB1008, doi:10.1029/2004GB002443, 2006.

Hofmann, D. J., Butler, J. H., Dlugokencky, E. J., Elkins, J. W., Masarie, K., Montzka, S. A., and Tans, P.: The role of carbon dioxide in climate forcing from 1979 to 2004: introduction of the Annual Greenhouse Gas Index, Tellus, 58(5), 614–619, 2006

Huang, J., Golombek, A., Prinn, R., Weiss, R., Fraser, P., Simmonds, P., Dlugokencky, E. J., et al.: Estimation of regional emissions of nitrous oxide from 1997 to 2005 using multinetwork measurements, a chemical transport model, and an inverse method, J. Geophys. Res., 113, D17313, doi:10.1029/2007JD009381 ,2008.

Huang, Y., Zou, J., Zheng, X., Wang, Y., and Xu, X.: Nitrous oxide emissions as influenced by anebdment of plant residues with different C:N ratios, Soil Biol. Biochem., 36, 973–981, 2004.

Intergovernmental Panel on Climate Change – Climate change 2007: The Physical Science Basis. Contribution of Working Group I to the Fourth Assessment Report of Intergovernmental Panel on Climate Change, edited by: Solomon, S., Qin, D., Manning, M., Marquis, M., Averyt, K., Tignor, M. M. B., Miller Jr., H. L., and Chen, Z. Cambridge University Press, Cambridge, UK, 95–127, 131–206, 501–546, 2007.

Jipp, P. H., Nepstad, D. C., Cassel, D. K., and De Carvalho, C. R.: Deep soil moisture storage and transpiration in forests and pastures of seasonally-dry Amazonia, Clim. Change, 39, 395–412, 1998.

Keller, M., Veldekamp, E., Weitz, A. M., and Reiners, W. A.: Pasture age effects on soil-atmosphere trace gas exchange in a deforested area of Costa Rica, Nature, 365, 244–246, 1993.

Kiese, R., Hewett, B., and Graham, A.: Seasonal variability of N_2O emissions and CH_4 uptake by tropical rainforest soils of Queensland, Australia. Global Geochem. Cy., 17, 1043, doi:10.1029/2002GB002014, 2003.

Knowles, R.: Denitrification, Microbiol. Mol. Biol. R., 46, 43–70, 1982.

Kroeze, C., Mosier, A., and Nouwman, L.: Closing the global N$_2$O budget: A retrospective analysis 1500–1994, Global Biogeochem. Cy., 13(1), 1–9, 1999.

Langenfelds, R. L., Francey, R. J., Pak, B. C., Steele, L. P., Lloyd, J., Trudinger, C. M., and Allison C. E.: Interannual growth rate variations of atmospheric CO$_2$ and its delta C-13, H-2, CH$_4$, and CO between 1992 and 1999 linked to biomass burning, Global Biogeochem. Cy., 16(3), 1048, 2002.

Maggiotto, S. R., Webb, J. A., Waggner-Riddle, C., and Thurtell, G. W.: Nitrous and nitrogen oxide emissions from turfgrass receiving different forms of nitrogen fertilizer, J. Environ. Qual., 29, 621–630, 2000.

Melilo, J., Steudler, P. A., Feigl, B. J., Neill, C., Garcia-Montiel, D. C., Piccolo, M. C., Cerri, C. C., and Tian, H.: Nitrous oxide emissions from forest and pastures of various ages in the Brazilian Amazon, J. Geophys. Res., 106, 34179-34188, 2001.

Miller, J. B., Gatti, L. V., D'Amelio, M. T. S., et al.: Airborne measurements indicate large methane emissions from the eastern Amazon basin, J. Geophys. Res., 34(10), L10809, doi:10.1029/2006GL029213, 2007.

Mosier, A., Kroeze, C., Nevison, C., et al.: Closing the global N$_2$O budget: nitrous oxide emissions trough the agricultural nitrogen cycle, Nutr. Cy. Agroecosys., 52, 225–248, 1998.

Neftel, A., Blatter, A., Schimid, M., et al.: An experimental determination of the scale lenght of N$_2$O in the soil of grass-land, J. Geophys. Res., 105, 12095–12103, 2000.

Neill, C., Steudler, P. A., Garcia-Montiel1, D. C., Melillo, J. M., Feigl, B. J., Piccolo, M. C., and Cerri, C. C.: Rates and controls of nitrous oxide and nitric oxide emissions following conversion of forest to pasture in Rondônia, Nutr. Cy. Agroecosys., 71, 1–15, 2005.

Oliver, J. G. J., Bouwman, A. F., Berdowski, J. J. M., Veldt, C., Bloos, J. P. J., Visschedijk, A. H. J., van de Maas, C. W. M., and Zandweld, P. Y. J.: Sectoral emission inventories of greenhouse gases for 1990 on per country basis as well as on 10 × 10, Environ. Sci. Pol., 2, 241–264, 1999.

Passianoto, C. C., Ahrens, T., Feigl. B. J., Steudler, P. A., do Carmo, J. B., and Melilo, J. M.: Emissions of CO$_2$, N$_2$O, and NO in conventional and no-till management oractices in Rondônia, Brazil, Biol. Ferlil Soils, 38, 200–208, doi:10.1007/s00374-003-0653-y, 2003.

Perez, T., Trumbore, S. E., Tyler, S. C., et al.: Isotopic variability of N$_2$O emissions from tropical forest soils, Global Biogeochem. Cy., 14, 525–535, 2000.

Prather, M. and Ehhalt, D.: Atmospheric chemistry and greenhouse gases: Climate Change 2001: The Scientific Basis, edited by: Houghton, J. T., Ding, Y., Noguer, M., van der Linden, P. J., et al., Cambridge University Press, New York, USA, 239–287, 2001.

Rosenkranz, P., Brüggemann, N., Papen, H., et al.: NO$_2$, NO and CH$_4$ exchange, and microbial N turnover a Mediterranean pine forest soil, Biogeosci. Discuss., 2, 121–123, 2005.

Ryden, J. C.: N$_2$O exchange between a grassland soil and the atmosphere, Nature, 292, 235–237, 1981.

Schindlbacher, A., Zechmeister-Boltenstern, S., and Butterbach-Bahl, K.: Effects of soil moisture and temperature on NO, NO$_2$ and N$_2$O emissions from European forest soils, J. Geophys. Res., 109, D17302, doi:10.1029/2004JD004590, 2004.

Smith, K. A., Ball, T., Conen, F., et al.: Exchange of greenhouse gases between soil and atmosphere interactions of soil physical factors and biological processes, Eur. J. Soil Sci., 54, 779–791, 2003.

Stehfest, E. and Müller, C.: Simulation of N$_2$O emissions from a urine-affected pasture in New Zealand with the ecosystms model DayCent, J. Geophys. Res., 109, D03109, doi:10.1029/2003JD004261, 2004.

Thiemens, M. H. and Trogler, W. C.: Nylon production – an unknown source of atmospheric nitrous-oxide, Science, 251, 932–934, 1991.

Van der Werf, G. R., Randerson, J. T., Collatz, G. J., Giglio, L., Kasibhatla, P. S., Arellano Jr., A. F. Olsen, S. C. and Kasischke, E. S.: Continental-Scale Partitioning of Fire Emissions During the 1997 to 2001 El Nino/La Nina Period, Science, 303(5654), 73–76, 2004.

Van Haren, J. L. M., Handley, L. L., Biel, K. Y., Kudeyarov, V. N., Mclain, J. E. T., Martens, D.A., Colodner, D. C.: Drought-induced nitrous oxide flux dynamics in an enclosed tropical forest, Global Change Biol., 11, 1247–1257, 2005.

Verchot, L. V., Davidson E. A., Cattannio J. H., et al.: Land use and biogeochemical controls of nitrogen oxide emissions from soils in eastern Amazonia, Global Biogeochem. Cy., 13, 31–46, 1999.

Wick, B., Veldkamp, E., de Mello, W. Z., Keller, M., and Crill, P.: Nitrous oxide fluxes and nitrogen cycling along a pasture chronosequence in Central Amazon, Brazil, Biogeosciences, 2, 175–187, 2005, http://www.biogeosciences.net/2/175/2005/.

Yamulki, S., Goulding, K. W. T., Webster, C. P., and Harisson, R. M.: Studies on NO and N$_2$O fluxes from a wheat field, Atmos. Environ., 29, 1627–1635, 1995.